International Journal of Applied Earth Observation and Geoinformation 44 (2016) 53–60

Contents lists available at ScienceDirect

International Journal of Applied Earth Observation and Geoinformation

journal homepage: www.elsevier.com/locate/jag

Short communication

Inter- and intra-annual variations of clumping index derived from the MODIS BRDF product

Liming He[a,*], Jane Liu[a,b], Jing M. Chen[a], Holly Croft[a], Rong Wang[a], Michael Sprintsin[c], Ting Zheng[a], Youngryel Ryu[d], Jan Pisek[e], Alemu Gonsamo[a], Feng Deng[f], Yongqin Zhang[g]

[a] Department of Geography and Program in Planning, University of Toronto, Toronto, ON M5S 3G3, Canada
[b] School of Atmospheric Sciences, Nanjing University, Nanjing 210093, China
[c] Forest Management and GIS Department, Jewish National Fund-Keren Kayemet LeIsrael, Eshtaol, M.P. Shimshon, 99775, Israel
[d] Department of Landscape Architecture and Rural Systems Engineering, Seoul National University, Seoul, Republic of Korea
[e] Tartu Observatory, Tõravere, 61602 Estonia
[f] Department of Physics, University of Toronto, Ontario, M5S 1A7, Canada
[g] Department of Biological Sciences, Delta State University, Cleveland, MS 38733 USA

ARTICLE INFO

Article history:
Received 27 April 2015
Received in revised form 23 July 2015
Accepted 24 July 2015
Available online 6 August 2015

Keywords:
Clumping index
MODIS
Seasonality
Variation
BRDF

ABSTRACT

Clumping index quantifies the level of foliage aggregation, relative to a random distribution, and is a key structural parameter of plant canopies and is widely used in ecological and meteorological models. In this study, the inter- and intra-annual variations in clumping index values, derived from the Moderate Resolution Imaging Spectroradiometer (MODIS) BRDF product, are investigated at six forest sites, including conifer forests, a mixed deciduous forest and an oak-savanna system. We find that the clumping index displays large seasonal variation, particularly for the deciduous sites, with the magnitude in clumping index values at each site comparable on an intra-annual basis, and the seasonality of clumping index well captured after noise removal. For broadleaved and mixed forest sites, minimum clumping index values are usually found during the season when leaf area index is at its maximum. The magnitude of MODIS clumping index is validated by ground data collected from 17 sites. Validation shows that the MODIS clumping index can explain 75% of variance in measured values (bias = 0.03 and rmse = 0.08), although with a narrower amplitude in variation. This study suggests that the MODIS BRDF product has the potential to produce good seasonal trajectories of clumping index values, but with an improved estimation of background reflectance.

© 2015 Elsevier B.V. All rights reserved.

1. Introduction

The spatial distributions of leaves in a canopy are often non-random because they are organized in various structures (Chen and Black, 1992). The non-randomness of leaf distribution can be quantified by a vegetation dispersion parameter called the clumping index (Ω) in a simple canopy radiation transfer model at a given zenith angle θ (Nilson, 1971):

$$P\left(\theta\right) = e^{-G(\theta)L\Omega(\theta)/\cos\theta} \quad (1)$$

where P is the gap fraction; G is a parameter describing leaf angular distribution and L is the leaf area index (LAI). If leaves of a canopy are randomly distributed, Ω is equal to 1. The Ω value can be larger than one when the foliage is regularly distributed. As leaves in a canopy become more clumped, Ω decreases, and its value is generally less than one. As optical vegetation indices are sensitive to effective LAI, Ω is used to convert the effective LAI to true LAI (Chen and Black, 1992). Leaf clumping affects radiation interception and distribution within canopies, consequently modulating evapotranspiration, energy partitioning and carbon uptake (Baldocchi and Harley, 1995; Chen et al., 2012). Consequently, Ω is identified as a key variable for describing canopy architecture within ecosystem models (Duthoit et al., 2008; Fang et al., 2013; Govind et al., 2013; Hill et al., 2011; Ryu et al., 2011; Sprintsin et al., 2011). In the two-leaf ecosystem models, Ω is used to accurately separate sunlit leaves from shaded leaves, and without considering foliage clumping, both the gross primary production and evapotranspiration estimates can be biased (Chen et al., in revision; Chen et al., 2012). Spatially-distributed information on the variability in Ω across different temporal scales, and for a range of ecosys-

* Corresponding author.
E-mail address: liming.he@gmail.com (L. He).

http://dx.doi.org/10.1016/j.jag.2015.07.007
0303-2434/© 2015 Elsevier B.V. All rights reserved.

tems, is therefore essential. However, retrieving the intra-annual variations of Ω from remotely sensed data, e. g. the Bidirectional Reflectance Distribution Function (BRDF) product of the Moderate Resolution Imaging Spectroradiometer (MODIS), is difficult because short-term fluctuations have been found in the derived Ω time series, implying that the Ω seasonality might be contaminated (He et al., 2012b).

The difficultly in modeling Ω from remotely-sensed data has led to relatively little research into retrieving spatially-continuous Ω values over large spatial extents. He et al. (2012b) produced a global Ω map at 500 m spatial resolution for one year (2006). However, they used a single annual-median value, therefore neglecting any potential seasonal variations in Ω. This study therefore focuses on investigating the magnitude and temporal trends of the seasonal variability of Ω for different vegetation types. Specifically, the objectives of this work are (1) to examine if the observed abrupt seasonal Ω fluctuations in the satellite data are caused by background changes due to rain events, (2) to examine the inter- and intra-annual variations of Ω for forested ecosystems, and (3) to quantify the magnitude of MODIS Ω (Ω_{MODIS}) values in mid-summer. For these purposes, we collect seasonal trajectories of Ω from ground measurements with several vegetation types and soil moisture data to identify noise in the Ω_{MODIS} time series; then we reconstruct the seasonality of clumping index using a smoothing algorithm; we analyze the reconstructed Ω_{MODIS} trajectories for multiple years and validate the magnitude of Ω_{MODIS} by ground data collected from 17 sites.

2. Methodology and data collection

2.1. Ground measurements of clumping index

For conifers, the Ω can be separated into two components (or scales), as either larger or smaller than the conifer shoot, which are measured in the field and in the laboratory, respectively (Chen, 1996):

$$\Omega\left(\theta_s\right) = \frac{\Omega_e\left(\theta_s\right)}{\gamma_e} \quad (2)$$

where θ_s is the solar zenith angle; Ω_e is the clumping of basic foliage elements larger than conifer shoots that can be indirectly measured by a field-based instrument; γ_e, the needle-to-shoot area ratio, accounts for clumping of needles within a shoot (Chen and Leblanc, 1997). For broadleaves, γ_e is assumed to be one if the foliage element is a single leaf. If the individual leaves are arranged in whorls or their petioles are very short, the identifiable foliage element might be larger than single leaf, and then the γ_e can be larger than one, as shown in the discussion section. When effective plant area index (PAI_e) (defined as one-half the total surface area of leaves and supporting woody materials per unit ground surface area) by LAI-2000 (LI-Cor Co.) in the middle of growing season, and L obtained from litter-fall data or allometry are available, Ω can also be estimated by solving the following equation (Chen, 1996):

$$L = (1-\alpha) \times PAI_e/\Omega \quad (3)$$

where α is the woody-to-total area ratio. Assuming that the measurements of PAI_e, L, and α are independent, the absolute error of Ω (σ_Ω, given as a standard deviation) is calculated as (Bevington and Robinson, 2003):

$$\left(\frac{\sigma_\Omega}{\Omega}\right)^2 \approx \left(\frac{\sigma \mathrm{PAI_e}}{\mathrm{PAI_e}}\right)^2 + \left(\frac{\sigma_L}{L}\right)^2 + \left(\frac{\sigma_\alpha}{1-\alpha}\right)^2 \quad (4)$$

We refer the derivation of Eq. (4) from https://en.wikipedia.org/wiki/Propagation_of_uncertainty

2.2. Clumping index from MODIS (Ω_{MODIS})

The individual Ω_{MODIS} for a specific time is retrieved from MODIS BRDF product (Schaaf et al., 2002) using the same method described in He et al. (2012b). A brief explanation is provided in the supplementary material. We combine the individual Ω_{MODIS}, corresponding hotspot, dark spot reflectance, and NDHD (Normalized Difference between Hotspot and Dark spot) into a time series and compare them with a soil moisture time series at the same locations, in order to identify Ω_{MODIS} noise possibly caused by rain events and changes in background. Here we choose soil moisture rather than precipitation and background reflectance because soil moisture data are available from flux tower sites; and for future application they are available from remote sensing (e. g. the Soil Moisture and Ocean Salinity (SMOS) mission and Soil Moisture Active-Passive (SMAP) mission). The noisy Ω_{MODIS} time series is then smoothed and reconstructed by a method named locally adjusted cubic-spline capping (LACC) (Chen et al., 2006).

2.3. Data collection

Ground measurements of Ω_e time series for 6 sites (4 conifer forest, 1 mixed forest, 1 oak-savanna) were collected from previous studies (Table 1) and used to calculate Ω (Eq. (2)) to compare to the seasonal Ω_{MODIS}.

The TP39 (42.71° N, 80.36° W), and TP74 (42.707° N, 80.348° W) sites in Ontario, Canada, are both needleleaf evergreen forests dominated by Mature White Pine (*P. strobus*) (Peichl et al., 2010). The RAdiation transfer Model Intercomparison (RAMI) pine site is dominated by Scots pine (*P. sylvestris* L.) stand in Järvselja, Estonia (58.31° N 27.30° E) (Kuusk et al., 2013). The Yatir site in Israel (31.35° N, 35.03° E), is a monocultured plantation which is dominated by Aleppo pine (*Pinus halepensis Mill.*) (Sprintsin et al., 2011). The Borden Forest site in Ontario, Canada (44.32° N, 79.93° W), a mixed deciduous forest from natural regrowth, is dominated by Red maple (*Acer rubrum* L.), Eastern white pine (*Pinus strobes* L.), Largetooth aspen (*Populus grandidentata Michx.*), and White ash (*Fraxinus Americana* L.) et al. (Froelich et al., 2015). The Tonzi ranch site, an oak-savanna ecosystem in California, USA (38.43° N; 120.96° W), is dominated by blue oak trees (*Quercus douglasii*) with occasional gray pines (*Pinus sabiniana*) (Baldocchi et al., 2004). (1) Tracing Radiation and Architecture of Canopies (TRAC) was used to measure Ω_e for a whole canopy at a given solar zenith angle (θ_s) along transects at TP39, TP74, Yatir, and Borden Forest sites (Chen and Cihlar, 1995); (2) Digital Hemispheric Photographs (DHPs) taken by fisheye lens under diffuse illumination conditions were used to retrieve Ω_e for the RAMI (Radiation transfer Model Intercomparison) pine site. Pisek et al. (2013) and Leblanc et al. (2005) provided detailed descriptions of the measurements and method used at this site, respectively; (3) At Tonzi Ranch site, the Ω_e was estimated from the upward-pointing digital images (Ryu et al., 2012) using the method of Macfarlane et al. (2007). The γ_e values for conifer species were collected from laboratory measurements (Chen et al., 1997) in this study or from literature.

To test if the median magnitude of Ω_{MODIS} over a whole season (He et al., 2012b) is in the reasonable range, we collected values of PAI_e, L and α from literature for 17 sites and used eq. (3) to calculate independent values of Ω as listed in Table 2.

Values for α were obtained from published data \(Supplemental material, Table 1) and a mean of 0.2 was used in the calculation of Ω. The MODIS BRDF product (MCD43A1) and corresponding data quality product (MCD43A2) from 2000 to 2013 were downloaded from Land Processes Distributed Active Archive Center (https://lpdaac.usgs.gov). We extracted the snow-free and high quality MODIS BRDF model parameters and derived Ω_{MODIS} for sites mentioned in Table 1 and Table 2. The soil moisture data (volumetric soil water

Table 1
Characteristics of the seven validation sites.

Site	Tonzi	RAMI pine	Yatir	TP39	TP74	Borden
Location	38.43°, −120.96°	58.31°, 27.30°	31.35°, 35.03°	42.71°, −80.36°	42.707°, −80.348°	44.319°, −79.934°
Forest type	MF	NEF	NEF	NEF	NEF	MF
Year of Sapling			1964–1969	1939	1974	Natural regrowth
Maximum LAI	0.84			~8	~7.5	4.6 in 2006
Overstory	GP <10% and BO	SP	AP	MWP	MWP	Red maple, large-tooth aspen, American beech
Understory	Grass	Sparse labrador tea and cotton grass, and a continuous sphagnum moss layer	Sparse grass in rain season (November–April)	Q. vultina, Abies balsamifera, Prunus serotina	*Q. vultina*, scattered patches of mosses	Dwarf shrubs, ferns and saplings
Tree height (m)	9.4 ± 4.3	16	~10	21.8 ± 1.7	13.1 ± 1.2	~20 m
Method	DHP: Macfarlane et al. (2007); Ryu et al. (2012)	DHP. Leblanc et al. (2005)	TRAC	TRAC	TRAC	TRAC
In-situ measurement	2009–2010	2011	2005, 2012, 2013	2011, 2012	2011, 2012	2013
Plot size	Every 30 m along three 300 m long transects 30 m apart	Flux tower site	Every 10 m along 100 m long transect	Every 10 m along 100 m long transect	Every 10 m along 100 m long transect	Every 10 m along 300 m long transect
γ_e	1	1.75	1.7	1.7	1.8	1
References	Baldocchi et al. (2004)	Kuusk et al. (2013)	Sprintsin et al. (2011)	Peichl et al. (2010)	Peichl et al. (2010)	Teklemariam et al. (2009)
Note			Thinning in 2012/2013 due to drought	Thinning in February 2012	No thinning	Forest species composition changes over years

Note: MF: Mixed Forest; NEF: Needleleaf Evergreen Forest; GP: Gray Pine (Pinus sabiniana); BO: Blue Oak (Quercus douglasii); SP: Scots Pine (*Pinus sylvestris L.*); AP: Aleppo Pine (*Pinus halepensis Mill.*); MWP: Mature White Pine (*P. strobus*); DHP: digital hemispherical photograph.

Table 2
Compilation of clumping index values from MODIS and from litter-fall collections and LAI-2000 measurements.

Site	Species	Year	Latitude	Longitude	LAI (Litterfall)	Le_max (LAI2000)	$\Omega \pm 1$SD ($\alpha = 0.20$)	Ω_{MODIS} (year)	References
Conifers:									
TP39[a]	White pine	2011	42.71	−80.360	7.23	5.37	0.59 ± 0.19	0.53 (2011)	this study
TP74[a]	White pine	2011	42.707	−80.348	6.18	4.01	0.52 ± 0.17	0.54 (2011)	this study
Yatir[b]	Aleppo pine	2001–2004	31.350	35.030	2.02	1.23	0.49 ± 0.16	0.59 (2003)	Sprintsin et al. (2011)
RAMI-Spruce[b]	Norway spruce	2007	58.295	27.256	6.76[g]	3.76	0.45 ± 0.15	0.54 (2006)	Kuusk et al. (2013)
RAMI-Pine[b]	Scots pine	2007	58.311	27.297	2.88[g]	1.75	0.49 ± 0.16	0.55 (2006)	Kuusk et al. (2013)
Metolius	Ponderosa pine	1997	44.499	-121.626	3.50	1.30	0.30 ± 0.10	0.48 (2006)	Law et al. (2001)
Broadleaved:									
RAMI-Birch	Silver and White birch	2007	58.281	27.331	3.93[g]	2.94	0.60 ± 0.10	0.69 (2006)	Kuusk et al. (2013)
Saskatchewan[c]	Aspen	1994–2003	53.630	−106.200	2.47		0.69 ± 0.11	0.68 (2006)	Barr et al. (2004)
Kannenbruch forest	Oak	2002	53.783	10.600	4.63	4.31	0.74 ± 0.12	0.69 (2006)	Kutsch et al. (2005)
Kannenbruch forest	Beech	2002	53.783	10.600	4.02	3.36	0.67 ± 0.11	0.69 (2006)	Kutsch et al. (2005)
Kannenbruch forest	Alder/Ash	2002	53.783	10.600	4.74	3.98	0.67 ± 0.11	0.69 (2006)	Kutsch et al. (2005)
Walker branch[d]	Oak	1995	35.958	−84.288			0.84 ± 0.14	0.71 (2006)	Baldocchi (1997)
Florida[e]	Cypress&slash pine	1996	29.783	−82.250			0.42 ± 0.07	0.54 (2006)	Liu et al. (1996)
Takayama[f]	Oak	2006	36.146	137.423	5.25	4.11	0.63 ± 0.10	0.65 (2006)	Nasahara et al. (2008)
Borden	Mixed species	1986	44.319	−79.934			0.53 ± 0.09	0.65 (2006)	Neumann and Denhartog (1989)
Costa Rica	Tropical dry forest	2001–2003	10.815	85.615	7.1	5.7	0.64 ± 0.10	0.68 (2006)	Kalacska et al. (2005)
Lausanne	European beech	2004	46.583	6.667	7.6	6.9	0.73 ± 0.12	0.68 (2006)	Thimonier et al. (2010)

Note: To calculate the uncertainty of Ω, we assumed that (1) the uncertainties of LAI from litterfall or allometry are 30% and 10% for conifers and broadleaved forests, respectively; (2) the uncertainty of Le is 10%; and (3) the uncertainty of woody-to-total area ratio is 8%. SD: standard deviation.

[a] Needle lifespan is set to 2 years old.

[b] Unit of SLA from the original literature is changed to half of total surface area of needle per weight.

[c] Corrected Le equals to LAI from litterfall using $\Omega = 0.69$.

[d] Assessed using radiative transfer data obtained from field site.

[e] Using equation: $Le = 0.53 \times L\_litter + 0.1$.

[f] The article authors suggested to check the shadow from mountain.

[g] The LAI is from allometric method.

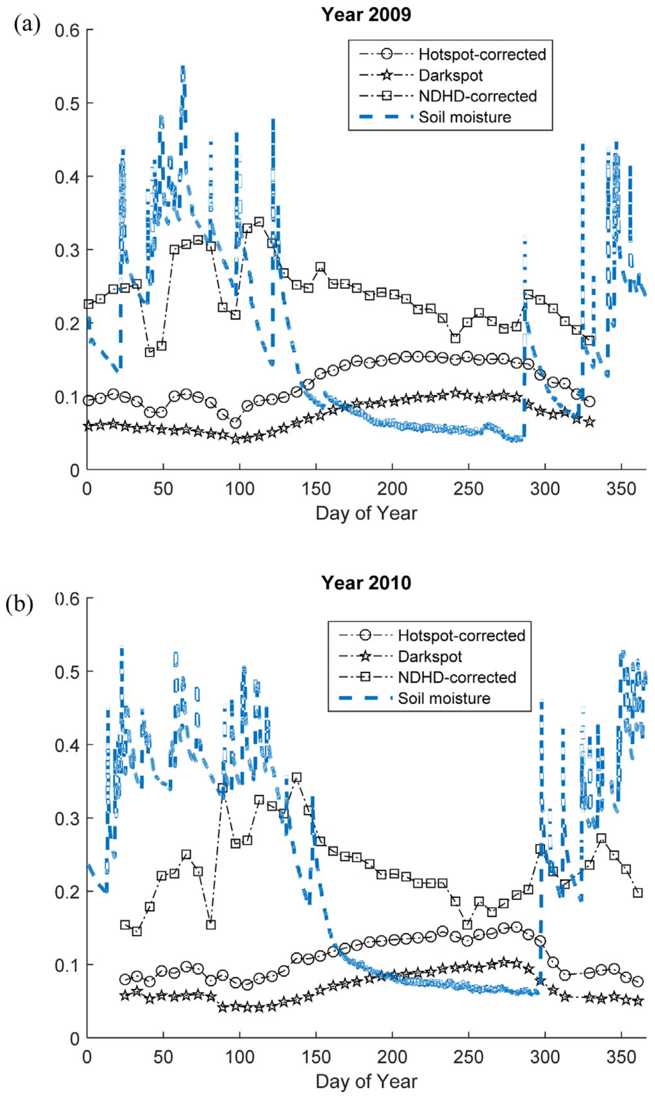

Fig. 1. Time series of the hotspot and dark spot reflectance (dimensionless), NDHD (dimensionless) derived from MODIS BRDF product (NDHD-corrected) and soil moisture (volumetric soil water content, m^3 m^{-3}) dynamics in top layers (0–15 cm) at Tonzi site in 2009 (a) and 2010 (b).

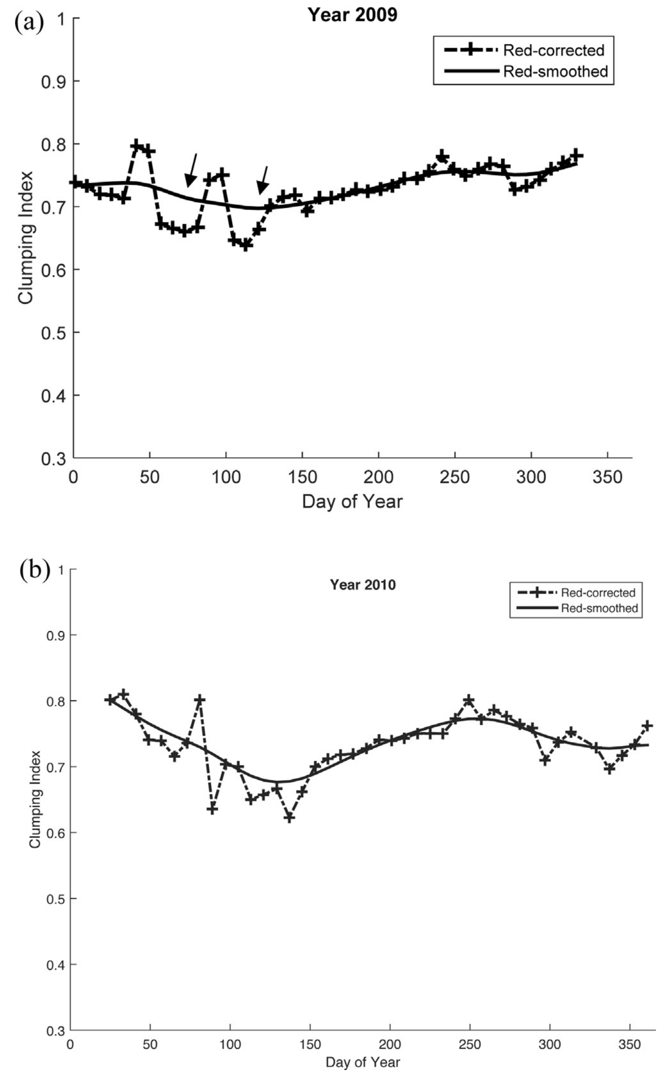

Fig. 2. Time series of clumping index derived from MODIS BRDF product for Tonzi site and the effect of smoothing algorithm. The dash-plus line is for original MODIS clumping index and the solid line is for the smoothed clumping index. The line around DOY 90 in 2009 (a) should go down further until the position indicated by the arrows.

content, %) of the top layers for Tonzi Ranch site (2001–2012) and Borden Forest (2005–2013) were collected and used to identify rain events and their potential impact on retrieval of Ω_{MODIS}.

3. Results

3.1. Reconstruction of the Ω_{MODIS} time series

The time series of the NDHD derived from MODIS BRDF product (NDHD-corrected) and soil moisture dynamics in the soil top layers across a complete growing season are first investigated. Fig. 1 shows an example time-series taken from the Tonzi site in 2009 and 2010.

The hotspot and dark spot values increase slowly from the beginning of year to ~DOY 280, mid-growing season, and then decrease slowly towards the end of year in 2009 and 2010. Short-term changes are found in the time series of the hotspot and dark spot reflectance values. These small changes in both the hotspot and dark spot are amplified in the NDHD time series and then transferred to Ω_{MODIS} (Fig. 2).

Many of these changes are directly related to sudden increases in soil moisture, which are caused by rain events; while the subsequent rain events do not change the previous background reflectance obviously. The actual change of Ω was tracked by MODIS: on DOY 286 in 2009, the study site experienced a storm with 40 mm rainfall and 10 m s^{-1} wind speed, the PAI was reduced by 30% (Ryu et al., 2012) and this resulted in a sudden decrease of Ω_{MODIS} followed by a nearly linear increase of Ω_{MODIS} during the following month (Fig. 2a). We also found that the decrease of NDHD around DOY 240 in 2009 and DOY 250 in 2010 (Figs. 1 and 2) cannot be explained by background change alone. For Borden Forest, it is also clear that the outliers in the NDHD values are associated with rain events identified from the abrupt changes of soil moisture (supplementary Fig. 1). These fluctuations of NDHD are also bounded by the rain events.

Fig. 2 also illustrates the effectiveness of the LACC method for noise removal in the Ω_{MODIS} time series. After evaluating the results for all site-years we find that the LACC method is successful in removing isolated noise; whilst for continuous noise (two or more continuous outliers), the LACC may take the noise as real signal. For example, the two increased points around DOY 40, and another two points around DOY 90 in the original Ω_{MODIS} curve (Fig. 2a) do not follow the general trend, and were not removed by the LACC

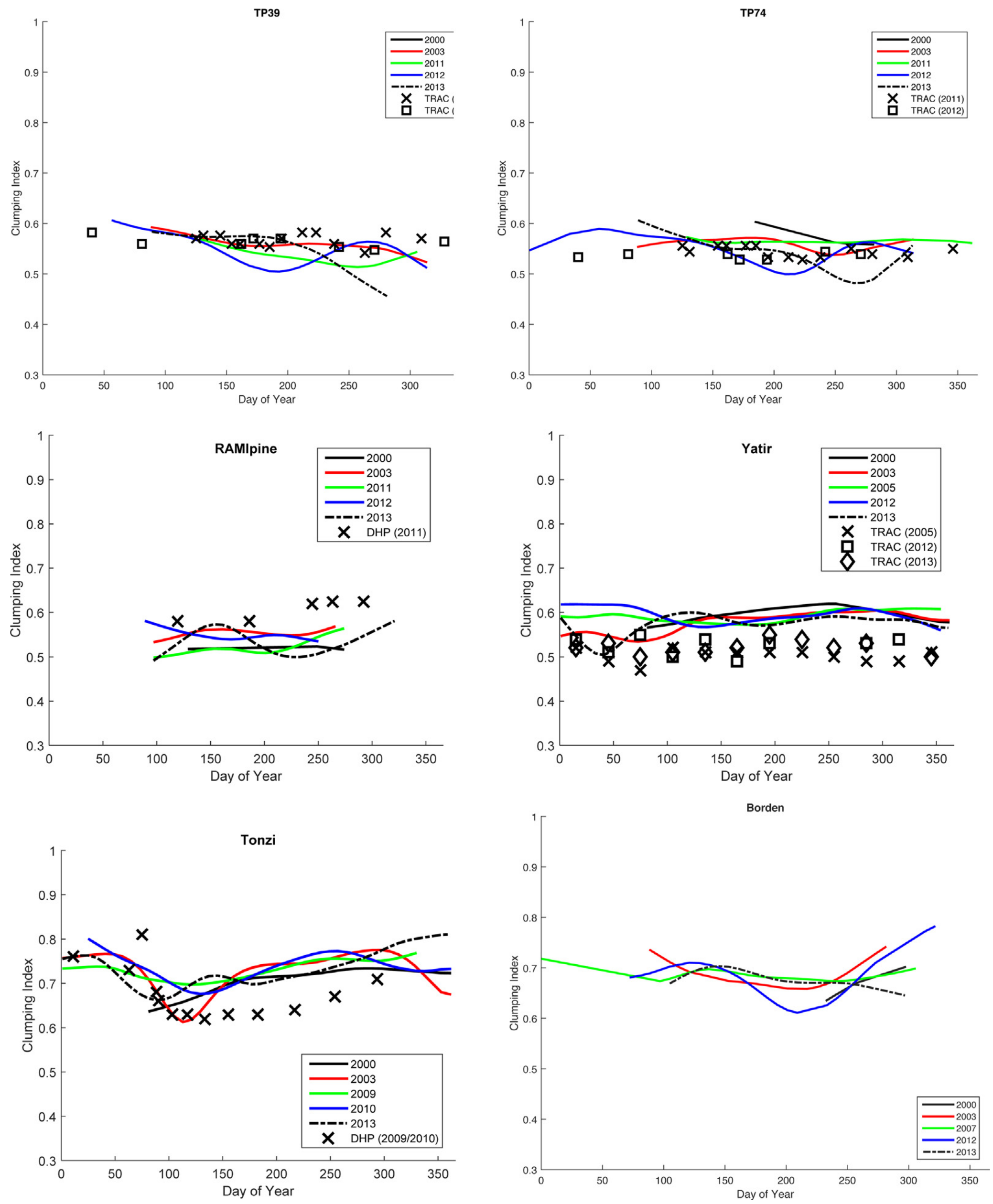

Fig. 3. Time series of smoothed Ω_{MODIS} for the six forest sites.

algorithm. In contrast to Fig. 2(a), the LACC method is capable to retain the decrease of Ω_{MODIS} in DOY 100–150 in 2010–during wet and growing season for oak-savanna system (Fig. 2b).

3.2. Inter- and intra-annual variations of Ω_{MODIS}

The Ω_{MODIS} time series at the six sites (Table 1) from 2000 to 2013 are derived from MODIS BRDF product and smoothed using LACC method. For clarity, we only show Ω_{MODIS} time series for years 2000 (the first complete year of Terra for the growing season), 2003 (the first year with both Terra and Aqua acquisitions), 2013 (the latest year) and the year(s) whenever ground measurements were available (Fig. 3).

For the four conifer sites (TP39, TP74, Järvselja, and Yatir), the inter- and intra-annual variations of Ω_{MODIS} are small, and consistent with the seasonality derived from ground measurements. The Ω_{MODIS} values for the TP39 and TP74 sites range between 0.5 and 0.6. In 2012, both the TP39 and TP74 sites show a similar decline of Ω_{MODIS} in the summer associated with a pronounced period of mid-summer hot and dry conditions (Trant, 2014). This decline is inconsistent with other years. This drop in NDHD values during the drought, is likely attributable to a decline in leaf chlorophyll resulting in an increase in the hotspot spot in the red band, and leading to higher NDHD and lower Ω_{MODIS} values. For the Järvselja RAMI Scots pine site, Ω_{MODIS} shows mostly small seasonality (0.52 to 0.57) because of low needle turnover rate (He et al., 2012a; Vestgarden, 2001). An increase in Ω_{MODIS} values around DOY 150 in 2013 is caused by two noisey data points in a row that could not be picked up by the LACC method (Supplementary Fig. 3). For the Yatir site, the Ω_{MODIS} values are ~0.6 which are close to the Ω derived from the Multi-angle Imaging SpectroRadiometer, by Pisek et al. (2013), but are higher than the multi-year TRAC measurements (assuming γ_e = 1.7 from literature). For the conifer sites, ground measured Ω values show good comparisons with the seasonality of Ω_{MODIS} values.

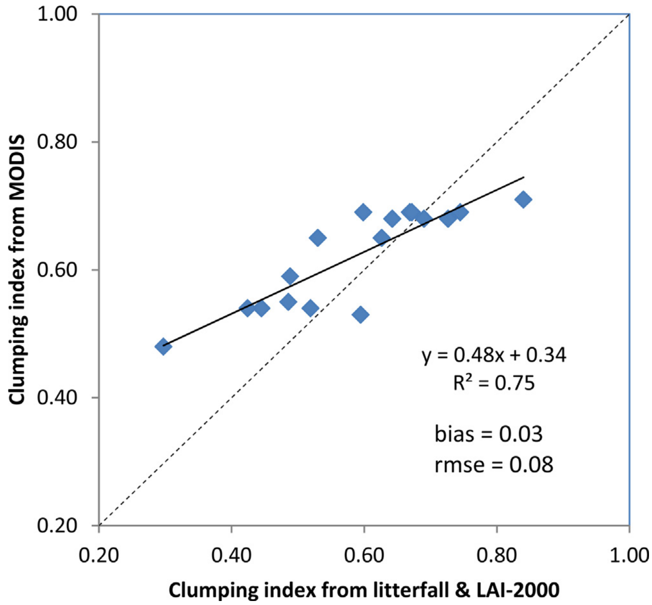

Fig. 4. The correlation between Ω_{MODIS} and $\Omega_{LAI\text{-}2000}$ (for site with forest canopy cover larger than 25%). Please refer to Table 2 for the uncertainty of clumping index from litter-fall & LAI-2000.

The Ω_{MODIS} in the Tonzi oak-savanna site ranges from 0.7 to 0.8 (Fig. 3), with a very consistent pattern among years: Ω_{MODIS} decreases from beginning of year to ∼DOY 120 when the LAI reaches its maximum, then increases slowly in the dry season until the beginning of rainy season in October. After that, Ω_{MODIS} decreases with time through the rainy season in winter. The pattern of Ω_{MODIS} is similar to results obtained by Ryu et al. (2012). The Ω_{MODIS} at the Borden mixed forest site shows a reasonable pattern with small seasonal variability (Fig. 3) Ω_{MODIS} ranges between 0.63 and 0.74, with minimum values occur in the summer when the canopy is usually the densest.. Although the species at Borden site are changing (Teklemariam et al., 2009), measurements taken approximately 25 years ago might provide a comparison for this old growth forest. According to measurements made in 1988 (Neumann and Denhartog, 1989) using the Markov model (Nilson, 1971), Ω at the same site (ranging from 0.46 to 0.67, during DOY 260-295) increases with decreasing LAI.

3.3. Comparison of Ω_{MODIS} with litter-fall collection and LAI-2000 measurements

A compilation of Ω values estimated using litter-fall collections and LAI-2000 measurements and the corresponding uncertainties is shown in Table 2.

We find that the Ω_{MODIS} explains 75% variance of clumping index derived from effective LAI and litter-fall collection of LAI ($p \ll 0.001$, bias = 0.03 and rmse = 0.08) (Fig. 4). The Ω_{MODIS} varies in a narrower amplitude than the Ω from these ground measurements. MODIS data agrees well with the ground measurements around the median values, but underestimates at higher, and overestimates at lower clumping index values. This is because satellite measurements respond to the structural effects near the top of the canopy, which is more clumped (He et al., 2012b); while the reflectance in red band tends to saturate for dense forest (higher LAI and γ_e,). This also suggests that the seasonality of forest Ω can be larger than has been shown from the MODIS retrieval.

4. Discussion

4.1. Background changes led to noise in Ω_{MODIS} retrieval

The results from this study found that precipitation led to changes in background reflectance, which introduced noise in the retrieved Ω_{MODIS} values for the forest sites. High soil moisture content leads to lower soil reflectance in red spectral band, and as the understory develops shortly after the start of rainy season at sparse sites, the total background reflectance in the red spectral band is decreased further (Ryu et al., 2010a). Whilst the forest canopy can be denser after the rain if new leaves appear, significant decreases of Ω_{MODIS} after rain events in the time series are likely noise.

4.2. Uncertainties in ground measurements of Ω

The modeled Ω_{MODIS} values were compared to the ground measurements in terms of both magnitude and seasonality, in order to validate the Ω_{MODIS} results. However, due to the compilation of ground data that was used from multiple sources, there may be significant discrepancies in the different ground measurement collection methods used to collect the data (Chen and Cihlar, 1995; Gonsamo and Pellikka, 2009; Leblanc et al., 2005; Leblanc and Fournier, 2014; Pisek et al., 2011). To quantify the uncertainty of Ω_{MODIS} in the middle-summer, we also calculated Ω from litter-fall collection and LAI-2000 measurements. It is understandable that the measured Ω values using eq. (3) are also prone to uncertainties due to errors related to α (Chen et al., 1997), LAI-2000 measurement (PAI_e) (Ryu et al., 2010b), and litter-fall collection (LAI).

5. Conclusions

The clumping index (Ω) and its seasonality are critical in global LAI mapping and ecosystem modeling. In this study, we investigate the inter- and intra-annual variations of Ω_{MODIS} derived from the MODIS BRDF parameter product. We found that the magnitude of Ω_{MODIS} at each site is comparable from year to year and the seasonality of Ω is well captured after noise removal. The seasonality of Ω_{MODIS} for conifer sites is very small and consistent with the ground measurements. For the broadleaved and mixed forest, i.e., Tonzi, and Borden Forest, the change of Ω_{MODIS} is driven by the phenology of leaves such as canopy thickening and defoliation, and the minimum Ω_{MODIS} is generally found in the season when LAI is the maximum. Ω_{MODIS} can explain 75% variation of Ω which is derived from litterfall collection and LAI-2000 measurements, although the variation of Ω_{MODIS} is smaller in amplitude than that of ground measurements. Ω_{MODIS} agrees well with the ground measurements around the median values, but underestimates clumping index at the high end and overestimates lower measured values, suggesting that the seasonality of forest Ω can be larger than the MODIS retrieval.

Acknowledgements

Dr. Kenlo Nishida Nasahara contributed the LAI-2000 and litterfall data at Takayama. We thank the AmeriFlux primary investigator (Dennis Baldocchi) of the Tonzi Ranch site in this study. Liming He was supported by the Canadian Space Agency grant (14SUSMAPTO). Jan Pisek was supported by Estonian Science Foundation Grant PUT232 'EST-SEEDS'.

Appendix A. Supplementary data

Supplementary data associated with this article can be found, in the online version, at http://dx.doi.org/10.1016/j.jag.2015.07.007

References

Baldocchi, D.D., Harley, P.C., 1995. Scaling carbon dioxide and water vapour exchange from leaf to canopy in a deciduous forest. II. Model testing and application. Plant Cell Environ. 18, 1157–1173.

Baldocchi, D.D., Xu, L.K., Kiang, N., 2004. How plant functional-type, weather, seasonal drought, and soil physical properties alter water and energy fluxes of an oak-grass savanna and an annual grassland. Agric. Forest Meteorol. 123, 13–39.

Baldocchi, D., 1997. Measuring and modelling carbon dioxide and water vapour exchange over a temperate broad-leaved forest during the 1995 summer drought. Plant Cell Environ. 20, 1108–1122.

Barr, A.G., Black, T.A., Hogg, E.H., Kljun, N., Morgenstern, K., Nesic, Z., 2004. Inter-annual variability in the leaf area index of a boreal aspen-hazelnut forest in relation to net ecosystem production. Agric. Forest Meteorol. 126, 237–255.

Bevington, P.R., Robinson, D.K., 2003. Data Reduction and Error Analysis for the Physical Sciences. McGraw-Hill, Boston.

Chen, J.M., Black, T.A., 1992. Foliage Area and Architecture of Plant Canopies from Sunfleck Size Distributions. Agric. Forest Meteorol. 60, 249–266.

Chen, J.M., Cihlar, J., 1995. Plant canopy gap-size analysis theory for improving optical measurements of leaf-area index. Appl. Opt. 34, 6211–6222.

Chen, J.M., Leblanc, S.G., 1997. A four-scale bidirectional reflectance model based on canopy architecture. Ieee T. Geosci. Remote 35, 1316–1337.

Chen, J.M., Rich, P.M., Gower, S.T., Norman, J.M., Plummer, S., 1997. Leaf area index of boreal forests: Theory, techniques, and measurements. J. Geophys. Res-Atmos. 102, 29429–29443.

Chen, J.M., Deng, F., Chen, M.Z., 2006. Locally adjusted cubic-spline capping for reconstructing seasonal trajectories of a satellite-derived surface parameter. Ieee T. Geosci. Remote 44, 2230–2238.

Chen, J.M., Mo, G., Pisek, J., Liu, J., Deng, F., Ishizawa, M., Chan, D., 2012. Effects of foliage clumping on the estimation of global terrestrial gross primary productivity. Global Biogeochem. Cycles 26.

Chen, B., Liu, J., Chen, J.M., Croft, H., Gonsamo, A., He, L., Luo, X., 2015. In revision. Assessment of foliage clumping effects on evapotranspiration estimates in forested ecosystems. Agric. Forest Meteorol.

Chen, J.M., 1996. Optically-based methods for measuring seasonal variation of leaf area index in boreal conifer stands. Agric. Forest Meteorol. 80, 135–163.

Duthoit, S., Demarez, V., Gastellu-Etchegorry, J.P., Martin, E., Roujean, J.L., 2008. Assessing the effects of the clumping phenomenon on BRDF of a maize crop based on 3D numerical scenes using DART model. Agric. Forest Meteorol. 148, 1341–1352.

Fang, H.L., Jiang, C.Y., Li, W.J., Wei, S.S., Baret, F., Chen, J.M., Garcia-Haro, J., Liang, S.L., Liu, R.G., Myneni, R.B., Pinty, B., Xiao, Z.Q., Zhu, Z.C., 2013. Characterization and intercomparison of global moderate resolution leaf area index (LAI) products: analysis of climatologies and theoretical uncertainties. J. Geophys. Res-Biogeo. 118, 529–548.

Froelich, N., Croft, H., Chen, J.M., Gonsamo, A., Staebler, R.M., 2015. Trends of carbon fluxes and climate over a mixed temperate-boreal transition forest in southern Ontario, Canada. Agric. Forest Meteorol. 211–212, 72–84.

Gonsamo, A., Pellikka, P., 2009. The computation of foliage clumping index using hemispherical photography. Agric. Forest Meteorol. 149, 1781–1787.

Govind, A., Guyon, D., Roujean, J.L., Yauschew-Raguenes, N., Kumari, J., Pisek, J., Wigneron, J.P., 2013. Effects of canopy architectural parameterizations on the modeling of radiative transfer mechanism. Ecol. Model. 251, 114–126.

He, L.M., Chen, J.M., Pan, Y.D., Birdsey, R., Kattge, J., 2012a. Relationships between net primary productivity and forest stand age in U. S. forests. Global Biogeochem. Cycles 26.

He, L.M., Chen, J.M., Pisek, J., Schaaf, C.B., Strahler, A.H., 2012b. Global clumping index map derived from the MODIS BRDF product. Remote Sens. Environ. 119, 118–130.

Hill, M.J., Román, M.O., Schaaf, C.B., Hutley, L., Brannstrom, C., Etter, A., Hanan, N.P., 2011. Characterizing vegetation cover in global savannas with an annual foliage clumping index derived from the MODIS BRDF product. Remote Sens. Environ. 115, 2008–2024.

Kalacska, M., Calvo-Alvarado, J.C., Sanchez-Azofeifa, G.A., 2005. Calibration and assessment of seasonal changes in leaf area index of a tropical dry forest in different stages of succession. Tree Physiol. 25, 733–744.

Kutsch, W.L., Liu, C.J., Hormann, G., Herbst, M., 2005. Spatial heterogeneity of ecosystem carbon fluxes in a broadleaved forest in Northern Germany. Global Change Biol. 11, 70–88.

Kuusk, A., Lang, M., Kuusk, J., 2013. Database of Optical and Structural Data for the Validation of Forest Radiative Transfer Models, Light Scattering Reviews 7. Springer, Berlin Heidelberg, pp. 109–148.

Law, B.E., Van Tuyl, S., Cescatti, A., Baldocchi, D.D., 2001. Estimation of leaf area index in open-canopy ponderosa pine forests at different successional stages and management regimes in Oregon. Agric. Forest Meteorol. 108 (1), 1–14.

Leblanc, S.G., Fournier, R.A., 2014. Hemispherical photography simulations with an architectural model to assess retrieval of leaf area index. Agric. Forest Meteorol. 194, 64–76.

Leblanc, S.G., Chen, J.M., Fernandes, R., Deering, D.W., Conley, A., 2005. Methodology comparison for canopy structure parameters extraction from digital hemispherical photography in boreal forests. Agric. Forest Meteorol. 129, 187–207.

Liu, S., Riekerk, H., Gholz, H.L., 1996. Leaf litterfall, leaf area index, and radiation transmittance in cypress wetlands and slash pine plantations in north-central Florida. Wetlands Ecol. Manage. 4, 257–271.

Macfarlane, C., Hoffman, M., Eamus, D., Kerp, N., Higginson, S., McMurtrie, R., Adams, M., 2007. Estimation of leaf area index in eucalypt forest using digital photography. Agric. Forest Meteorol. 143, 176–188.

Nasahara, K.N., Muraoka, H., Nagai, S., Mikami, H., 2008. Vertical integration of leaf area index in a Japanese deciduous broad-leaved forest. Agric. Forest Meteorol. 148, 1136–1146.

Neumann, H.H., Denhartog, G., 1989. Leaf-area measurements based on hemispheric photographs and leaf-litter collection in a deciduous forest during autumn leaf-Fall. Agric. Forest Meteorol. 45, 325–345.

Nilson, T., 1971. A theoretical analysis of the frequency of gaps in plant stands. Agric. Meteorol. 8, 25–38.

Peichl, M., Arain, M.A., Brodeur, J.J., 2010. Age effects on carbon fluxes in temperate pine forests. Agric. Forest Meteorol. 150, 1090–1101.

Pisek, J., Lang, M., Nilson, T., Korhonen, L., Karu, H., 2011. Comparison of methods for measuring gap size distribution and canopy nonrandomness at Järvselja RAMI (RAdiation transfer Model Intercomparison) test sites. Agric. Forest Meteorol. 151, 365–377.

Pisek, J., Ryu, Y., Sprintsin, M., He, L.M., Oliphant, A.J., Korhonen, L., Kuusk, J., Kuusk, A., Bergstrom, R., Verrelst, J., Alikas, K., 2013. Retrieving vegetation clumping index from-Multi-angle Imaging SpectroRadiometer (MISR) data at 275 m resolution. Remote Sens. Environ. 138, 126–133.

Ryu, Y., Baldocchi, D.D., Verfaillie, J., Ma, S., Falk, M., Ruiz-Mercado, I., Hehn, T., Sonnentag, O., 2010a. Testing the performance of a novel spectral reflectance sensor, built with light emitting diodes (LEDs), to monitor ecosystem metabolism, structure and function. Agric. Forest Meteorol. 150, 1597–1606.

Ryu, Y., Nilson, T., Kobayashi, H., Sonnentag, O., Law, B.E., Baldocchi, D.D., 2010b. On the correct estimation of effective leaf area index: Does it reveal information on clumping effects. Agric. Forest Meteorol. 150, 463–472.

Ryu, Y., Baldocchi, D.D., Kobayashi, H., van Ingen, C., Li, J., Black, T.A., Beringer, J., van Gorsel, E., Knohl, A., Law, B.E., Roupsard, O., 2011. Integration of MODIS land and atmosphere products with a coupled-process model to estimate gross primary productivity and evapotranspiration from 1km to global scales. Global Biogeochem. Cycles 25 (GB4017), http://dx.doi.org/10.1029/2011GB004053

Ryu, Y., Verfaillie, J., Macfarlane, C., Kobayashi, H., Sonnentag, O., Vargas, R., Ma, S., Baldocchi, D.D., 2012. Continuous observation of tree leaf area index at ecosystem scale using upward-pointing digital cameras. Remote Sens. Environ. 126, 116–125.

Schaaf, C.B., Gao, F., Strahler, A.H., Lucht, W., Li, X.W., Tsang, T., Strugnell, N.C., Zhang, X.Y., Jin, Y.F., Muller, J.P., Lewis, P., Barnsley, M., Hobson, P., Disney, M., Roberts, G., Dunderdale, M., Doll, C., d'Entremont, R.P., Hu, B.X., Liang, S.L., Privette, J.L., Roy, D., 2002. First operational BRDF, albedo nadir reflectance products from MODIS. Remote Sens. Environ. 83, 135–148.

Sprintsin, M., Cohen, S., Maseyk, K., Rotenberg, E., Grunzweig, J., Karnieli, A., Berliner, P., Yakir, D., 2011. Long term and seasonal courses of leaf area index in a semi-arid forest plantation. Agric. Forest Meteorol. 151, 565–574.

Teklemariam, T., Staebler, R.M., Barr, A.G., 2009. Eight years of carbon dioxide exchange above a mixed forest at Borden, Ontario. Agric. Forest Meteorol. 149, 2040–2053.

Thimonier, A., Sedivy, I., Schleppi, P., 2010. Estimating leaf area index in different types of mature forest stands in Switzerland: a comparison of methods. Eur. J. Forest Res. 129, 543–562.

Trant, J.S., 2014. Effects of Thinning on Carbon Dynamics in a Temperate Coniferous Forest. McMaster University.

Vestgarden, L.S., 2001. Carbon and nitrogen turnover in the early stage of Scots pine (*Pinus sylvestris* L.) needle litter decomposition: effects of internal and external nitrogen. Soil Biol. Biochem. 33, 465–474.